

## Electron Paramagnetic Resonance from Clean Single-Crystal Cleavage Surfaces of Silicon\*

D. HANEMAN†

*Department of Physics, Brown University, Providence, Rhode Island 02912*

(Received 30 November 1967)

EPR measurements have been made on aligned cleavage faces of Si, prepared and studied in high vacuum ( $<10^{-9}$  Torr). The signal, observable after accumulation, is a single line at  $g=2.0055$  with width 6 G, similar to that from vacuum-crushed powders. It is unaffected by oxygen exposures below  $10^{-8}$  Torr min, known to affect the work function and surface-region conductivity, but is increased in height (45%) and number of spins (20%) by heavy oxygen exposures in the range  $10^{-1}$  Torr min and above. Hyperfine structure or  $g$  anisotropy is not resolved. The surface density of spins is approximately  $8 \times 10^{18}$  cm $^{-2}$ . Comparisons with other measurements of effects of oxygen on surface-region conductivity and work function show that the resonance centers are located on the surface. Analysis of the resonance, in particular the limited hyperfine structure and  $g$  isotropy, shows that the unpaired electrons are largely nonlocalized and in a conduction band of large effective mass whose maximum anisotropy in reciprocal lattice space is little more than that along a single axis of the bulk conduction band. A model for the surface structure is proposed which is consistent with both the EPR data and low-energy electron diffraction measurements of surface-structure symmetry. Alternate rows of close-spaced atoms are raised with  $s$ -type dangling bonds which overlap about 80%, forming conduction rows. The remaining alternate rows are depressed, having  $p$  dangling bonds which overlap fully and do not contribute to the resonance. The rows have a preferred direction related to the progression of the crack that caused the cleavage. The on-surface conductance is predicted to be anisotropic, the highest value being along the rows. A possible identification of these  $s$  and  $p$  bands, with surface-state bands is suggested.

### I. INTRODUCTION

THE display of paramagnetic resonance by silicon after crushing, sandblasting, or polishing has raised the question of the nature and origin of the resonance centers. Originally, the resonance at  $g=2.0055$  had been ascribed to some unspecified kind of defect introduced near the surface during the mechanical treatment.<sup>1</sup> More recently, it was shown that the resonance from silicon crushed in ultrahigh vacuum was strongly affected by exposure to gases, causing alterations in line shape, height, width, and sensitivity to temperature changes.<sup>2</sup> It was concluded that the centers were most likely on the surface itself, being identified as the unpaired bonds caused on rupture of the material during crushing or abrasion. In view of the great interest in silicon surfaces, it is of importance to establish whether unpaired bonds are in fact present on clean surfaces produced by rupture or cleavage. This is of significance both in understanding the electrical properties and in elucidating the surface structure which has not yet been firmly established, although low-energy electron diffraction (LEED) and other measurements have been made.

Although the study of crushed powders is advantageous in that sufficient area is obtainable to give an easily observed resonance, there are objections to the use of this method. The process of crushing, while controllable macroscopically, may introduce violent combinations of stresses on a microscopic scale, which raises the

suspicion that mechanical damage, in addition to simple fragmentation, might be taking place. Furthermore, although the surfaces exposed are mainly the (111) cleavage faces, the multiplicity of orientations of these faces may average out anisotropy and mild hyperfine structure. No such structure was observed in the powder resonance and although the anisotropy, if it is present, is still obtainable in principle from a powder signal, it may be hidden by the linewidth if the anisotropy and splitting are small. Much better resolution is obtainable from parallel oriented faces.

To avoid the above objections, it was decided to study clean aligned single-crystal cleavage surfaces. If the cleavages were performed in ultrahigh vacuum in a manner similar to that used to study LEED and other surface properties, direct comparison of results would be facilitated. Furthermore, the stresses administered to the material in a properly applied cleavage technique are close to the minimum necessary to split the material, thus minimizing the complex and heavy stress combinations possibly present during crushing. Additionally, the orientation of a good cleavage face is fairly well defined.

Unfortunately, the signal strength is low. From the previous work with powders, it was estimated that 1 cm $^2$  of surface area would give a signal within a factor of 2 of the noise in a spectrometer of nominal  $2 \times 10^{11}$  spins/G sensitivity. However, by the use of signal accumulation techniques, sufficient improvement in the signal-to-noise ratio was possible.

### II. METHOD

From preliminary trials on cleavage faces, it was found necessary, even with accumulation techniques, to have more than 0.5 cm $^2$  of surface in the EPR cavity

\* Research supported by National Science Foundation and Advanced Research Projects Agency under Contract No. SD-86.

† National Science Foundation, Senior Foreign Scientist Fellow. Present address: School of Physics, University of New South Wales, Sydney, Australia.

<sup>1</sup> G. K. Walters and T. L. Estle, *J. Appl. Phys.* **32**, 1854 (1961).

<sup>2</sup> M. F. Chung and D. Haneman, *J. Appl. Phys.* **37**, 1879 (1966).

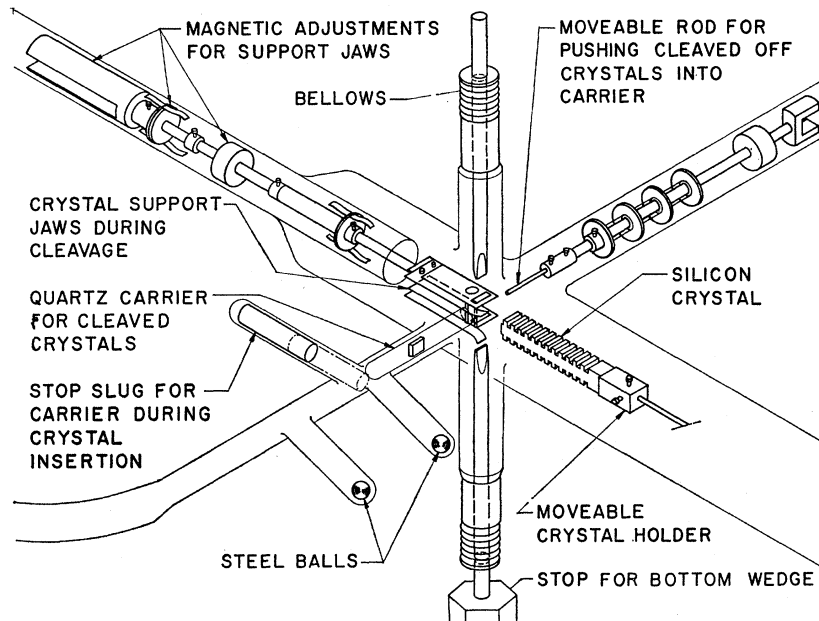


FIG. 1. Diagram of cleavage apparatus. The carriage controlling crystal motion is not shown.

in order to obtain a satisfactory signal. However, the production (in vacuum) of single cleavage areas of this magnitude of suitable flatness and with reasonable reliability was difficult. The best techniques for obtaining large areas involved use of wedges in prepared grooves so that the over-all specimen size was even larger than the cleavage face. Further, in an X-band spectrometer the microwave magnetic flux in the  $TE_{012}$  cavity available is concentrated within a few millimeters of the axis of maximum flux, so that there is little advantage in using specimens that exceed this region. In addition, excess Si in the cavity lowers the  $Q$  and sensitivity undesirably.

From considerations such as these, it was found best to cleave several smaller pieces and stack them parallel in the cavity. The space around the cavity is restricted both by the magnet pole faces and the waveguide, so that the cleavage and crystal slice alignment operations had to be performed in a portion of the vacuum system which was at some distance from the narrow quartz tube that was to be inserted into the cavity. Other restrictions on the design involved the necessity to move the cloven crystals into the small tube without con-

tamination, such as caused by friction, and to place the tube into the cavity through its vertical hole without disconnection from the vacuum system.

The necessary conditions were fulfilled by making the entire system portable, to allow approach to the EPR system after vacuum processing. The framework of dexion supporting the vacuum envelope could be raised and lowered 8 in. by rotating four threaded support legs, which screwed into threaded socket supports on the framework. The four rods were rotated via sprockets coupled to a motor driven chain, all of which was attached to a solid base plate. In this way the quartz appendage tube which would carry the crystals could be very carefully inserted into the microwave cavity by lowering the whole vacuum system. The front portion of the base of the bakeout oven was hinged and dropped down out of the way to allow access to the cavity and insertion of the tube in the cavity. The EPR magnet surrounding the cavity protrudes an amount approximately equal to the length of the hinged base plate. This determines the length of the tube connecting the main vacuum system with cleavage apparatus to the quartz appendage tube.

A schematic diagram of portion of the crystal cleavage arrangements is shown in Fig. 1, and details of the crystal support during cleavage are shown in Fig. 2. The crystal with prepared grooves is moved forward by a magnetically operated screw drive (not shown) into the stainless-steel support jaws. These are provided with thin stops, as shown in Fig. 2, which bear against the edges of the crystal. The molybdenum wedges are carefully inserted into opposite slots on the crystal, and the bottom wedge is supported in position by an external adjustable stop. The top wedge is given an appropriate impulsive blow from outside. This causes a crack be-

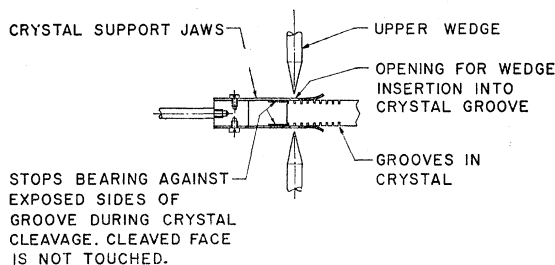


FIG. 2. Detail of support of crystal during cleavage.

tween the grooves. The wedges are released, the bulk crystal is withdrawn slightly, and the now freed, cleaved-off slice is pushed by a molybdenum side rod into a small quartz tube, the quartz "carrier," which is in exact position to receive the slice.

In practice, the first slice is discarded because its front face is an etched one. Also, any slices that do not cleave satisfactorily are discarded. The process is repeated by bringing forward the bulk crystal again, until three good slices are stacked in the quartz carrier. This is shown in detail in Fig. 3, illustrating the internal quartz side pieces that ensure parallel alignment of the slices. Next, the nickel stop slug backing the quartz carrier during crystal insertion is pulled away, and the quartz carrier is pushed out of the retaining clip on the crystal support jaws. A steel ball is brought out (magnetically) to the front of the carrier and pushes the carrier along the glass tube to the end. This avoids any rubbing on the crystals during transport. Here the quartz carrier makes a 90° turn in a specially designed chamber and drops into the 11-mm-o.d. quartz EPR tube, the slight fall being cushioned by the glass wool pad at the bottom, as shown Fig. 3. The vacuum system is then lowered so that the EPR tube enters the top opening of the microwave cavity and sinks until the Si crystals are in the center of the cavity. The portion of the quartz appendage tube with the glass wool is below the bottom of the cavity where it cannot contribute to the resonance.

### III. CRYSTAL AND TUBE PREPARATION

Since the signal was so weak, great care had to be exercised to minimize cavity, quartz, and other background signals. It was possible to clean the cavity so that its background was not significant after signal accumulation. However, the quartz carrier, even after prolonged etching, was a source of resonances of a magnitude comparable to the noise level and therefore not much less than the Si resonance. Efforts to reduce the quartz background still further were not successful. However, removal of the quartz carrier was not as helpful as one might expect, since the presence of the quartz bulk in close proximity to the crystal acted as a microwave field concentrator, giving an effective intensity gain by a factor of 3. Loss of this factor was not worthwhile. Eventually, the best compromise was to retain the carrier as shown in Fig. 3.

It was essential that no signal be obtained from the crystal itself prior to cleavage. Possible sources were the prepared sides of the 5×4×30-mm crystal (floating zone, *n* type, (111) axis, 500–3000 Ω cm, lifetime ~6 μsec) and of the grooves, since abraded surfaces give an EPR signal. After cutting with a diamond wheel, the crystal was polished to size with successively finer grades of polish, taking into account known damage depths.<sup>3</sup> The grooves, approximately 14 mil wide and

<sup>3</sup> A. Taloni and D. Haneman, *Surface Sci.* 8, 323 (1967).

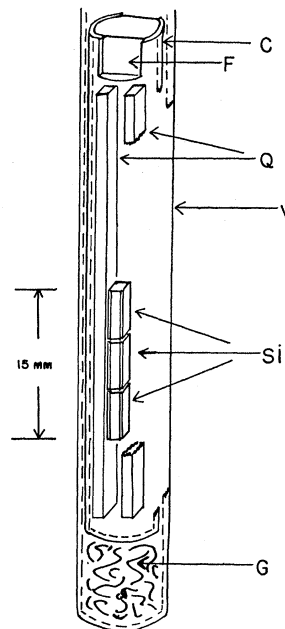


FIG. 3. Diagram of crystals aligned by quartz slabs inside quartz carrier tube. Latter rests on glass wool pad inside quartz appendage tube. Pad region is below cavity during measurement.

20 mil deep, were cut with a carborundum wheel, parallel to (111) planes, so that the subsequent crack was (111) oriented. The crystal was etched in CP4 acid so as to remove 1½–2 mil from each surface. Tests on separate slices (Fig. 4) showed that after accumulation no signal was detectable from surfaces which were given the above treatment. As a further check, a crystal after cleavage and EPR measurement in air was given an etch on portion of the cleaved faces. A drop of acid was carefully placed on one face so that none would spread onto the edges or into the exposed groove. The acid was then washed off, after estimating the area that was etched, and the crystal rinsed. A drop of acid was placed

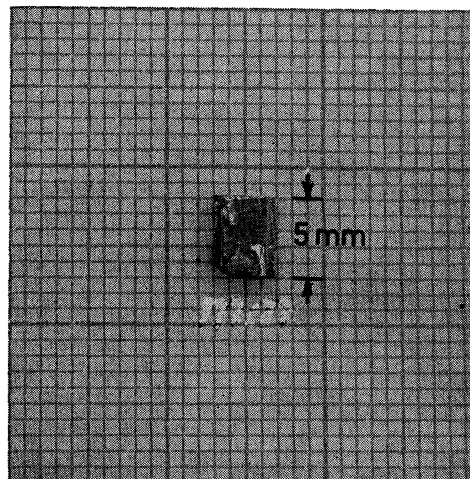


FIG. 4. Photograph of cleavage face showing some steps.

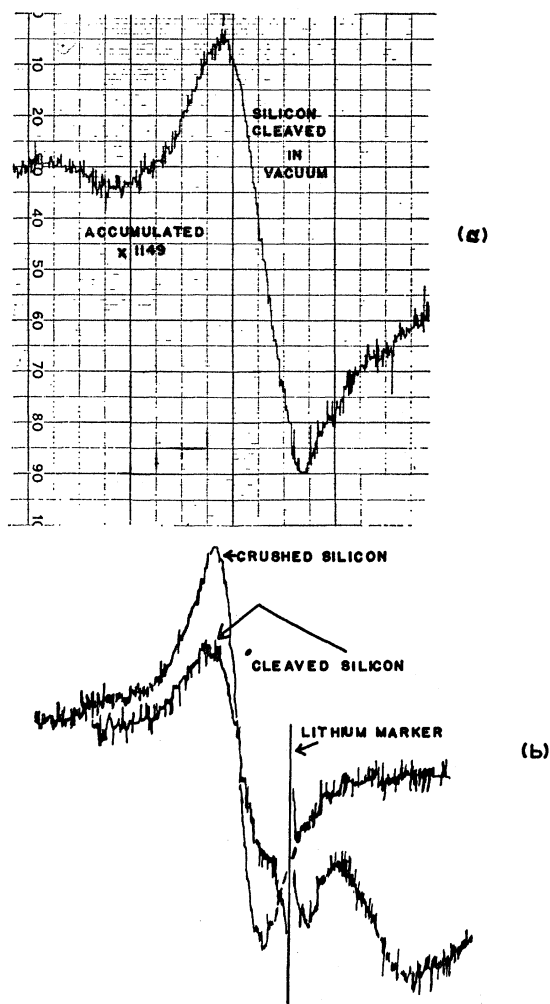


FIG. 5. (a) General appearance of signal from aligned cleaved Si after accumulation. (b) Signals from cleaved crystals and crushed powder superimposed, using Li marker signal on each trace as correspondence mark. Quartz background is visible on cleaved crystal signal in marker region.

on the second face and rinsed off. It was estimated that approximately 60–80% of the cleavage surface was etched. The signal was reduced by 65%. (The error in estimating the etched area was at least 10% and perhaps 20%, due to the contours of the acid drop and to the steps on the surface.) The result of this test was therefore consistent with the signal being due to the cleavage surfaces. A further check was made by comparing the signal from a normal slice with one which cleaved with two wedge-shaped edges. The areas of cleaved surface on the two specimens were approximately the same, but the first specimen had approximately three times the area of polished and etched surface on its edges. The signal strengths from the two specimens were, however, closely similar, again in accord with the signal coming from the cleavage surfaces.

Other precautions were necessary. During cleavage in the main tube, occasional small splinters of crystal

were formed. These were almost all retained in the main tube. However, on one occasion fragments were observed in the carrier. These fell to the bottom of the carrier when it dropped into the EPR tube and were then below the bottom of the cavity during measurement. Careful inspection showed no fragments in the portion of quartz carrier which was in the cavity. Repetitions of the experiment with fresh sets of crystals gave signals of comparable magnitudes, reconfirming that the resonance came from the cleavage faces. Background was of course tested in the absence of only the crystals.

The necessity for this care was occasioned both by the small size of the signal and also by the initially unexpected, though subsequently explicable, nature of the results.

The vacuum system was pumped by a three-stage diffusion pump, with special glass baffles, isolated by a bakeable valve, and a 30-liter/sec getter ion pump, with usual bakeout and cleaning procedures. Gases were admitted through metal valves. An ionization gauge was mounted midway along the glass extension tube leading to the quartz EPR tube. At low emission, its pressure readings were four times higher than those deduced from the pump current ( $\sim 1 \times 10^{-10}$  Torr).

#### IV. ACCUMULATION AND MEASUREMENT

A Varian X-band spectrometer with 6-in. magnet and 100-kc/sec modulation was used for the EPR measurements. Modulation amplitude was usually 1.4 G, and microwave power attenuation was 10 or 3 dB (no saturation). Signal accumulation in 1024 channels was performed with a CAT (Computer of Average Transients, Technical Measurement Corporation) connected to the spectrometer output. A repetitive magnet sweep of 60 G was obtained from an external synchronous motor and an endless potentiometer arrangement, which triggered the accumulation cycle on and off at fixed points relative to the magnet sweep. Since this was independent of the signal, the system of measurement was subject to frequency and field drift in the spectrometer. Such was detectable within a few hours of switching on the spectrometer. However, after attaining equilibrium, the system was remarkably stable, and the width of the signal after an accumulation of up to two days was the same as that

TABLE I. Measurement of signal height for different accumulation conditions. Result  $R = h \times VR \times \text{Rec} / [(100 \text{ mV}) \times G \times N]$ .

Amplifier recorder gain $G$	Height of trace $h$	CAT voltage range $VR$	Recorder range $\text{Rec}$	No. of accumulations $N$	Results $R$
8000	63	$3.3 \times 10^3$	1 V	2658	0.978
8000	43	330	1 V	180	0.987
6300	23	$3.3 \times 10^3$	1 V	1248	0.965
6300	75	$10^3$	1 V	1248	0.955
6300	74	$10^4$	100 mV	1248	0.944

after 20 min, to within the measurement accuracy, in the presence of noise at the peaks, of about 0.4 G (signal width  $\sim 5\frac{1}{2}$  G). Drift of usually less than about  $\frac{1}{2}$  G was confirmed by observation of a narrow Li metal signal, of width less than 1 G. After it was found from tests, soon after cleavage, that the signal, a single line, as shown in Fig. 5(a), was not altered by standing for many hours in the vacuum, all accumulations were repeated for different times and read out on a recorder using the different range scales on the CAT output, necessitated by the different accumulation times. Some results are shown in Table I.

The last column  $R$  shows the deduced height (multiplied by an arbitrary factor) for different settings of various ranges necessitated from using different numbers of accumulations. The last three rows show the effect, for a single accumulation, of reading the output for different CAT and recorder range settings. The values, which should ideally be the same, range from 0.944 to 0.978. This was about the largest span noted; often the readings corresponded to within 2% or less than 1%. Therefore signal height readings were regarded in general as accurate to within at least 5%. Signal width measurements involved accurate determinations of peak centers in the presence of noise and possible distortion due to background. Repeated measurements of the same signal under different accumulation and display conditions gave readings of  $19\frac{1}{2}$ – $20\frac{1}{2}$  units, and width measurements were therefore regarded as accurate to 5%.

A point about scanning speed and width may be made. Theoretically, if the time constant of the detector output is matched to a single output scan, one slow scan should give the same signal-to-noise as an accumulation of many scans during this time. (Signal-to-noise improves with the square root of the number of accumulations.) However, in practice, accumulation is preferable because it allows constant monitoring of the signal which can be read at any time. This is important in tuning and adjustment operations or during gas exposures, for all of which time may be of the essence in work of this kind. Without accumulation it would be necessary to choose a time constant in advance which one cannot predict optimally for various conditions. Similar considerations influence the choice of sweep rate. In general, the faster the sweep the more convenient the system, consistent with power supply characteristics. In this work a scan of 20 sec for 60 G was found convenient, the output being accumulated for 16 sec of each scan, the remaining time being used to allow the magnet power supply to return to the starting point and consequent surges to die away.

## V. RESULTS

In the absence of accumulation a signal (knowing where to look) was barely detectable above the noise at  $g=2.0055$ . After accumulation it had the general

appearance shown in Fig. 5. Accumulations were carried out at other regions of the magnetic field and small signals sometimes appeared but these, unlike the signal at  $g=2.0055$ , were invariably found to be independent of the presence of the silicon crystals. If signals due to the silicon were present at values far removed from  $g=2$ , they were not found and would be very small. They have not been detected for vacuum-crushed powders.

As can be seen the resonance appears to be a single line. Both orientation and gas exposure tests were made. For these a Li metal marker was incorporated in the form of a very small dot held on a small strip of adhesive tape. This was inserted until the dot just entered the cavity. In this way the normally very intense Li signal was kept small enough so as not to interfere unduly with the Si resonance.

The cleavage faces were not mirror flat but included steps and regions which were conchoidal near the edges. A typical face is shown in Fig. 4. The orientation of the facets on a microscopic scale is the important factor. Since the (111) is the favored cleavage plane, most of the facets even in the conchoidal regions are (111), with some (110) and other content, especially on the sides of steps which, as shown in the case of Ge,<sup>4</sup> are non-crystallographic. It is estimated from examination of the crystals that over 90% of the surfaces consisted of (111) regions.

### A. Orientation Studies

With the crystals placed parallel to within a few degrees, the signal was measured as the EPR tube was rotated about its (vertical) axis. This had to be done after disconnection of the tube from the main system. One test was made after exposure of the crystals to air and with the glass connection broken. The other test was performed on the clean surfaces after sealing off a well out-gassed section of the tube near the end under high vacuum. One axis of rotation was [110] and the other one which was used, applying to crystals cut at right angles to the others, was [112]. The traces (after accumulation) showed no established change of the Si signal with respect to the Li marker, as a function of orientation. Measurements were made at 30° intervals of rotation with various intermediate angles in addition. The absence of observable rotation effects was consistent with the fact that the over-all width and  $g$  value of the single-crystal resonance appeared to be the same as for the crushed powder. The traces for both, after passing through the accumulation system, were superimposed using the Li marker as correspondence point. As shown in Fig. 5(b), the width and  $g$  value are observably the same, even in the presence of a quartz background signal just beyond the lower peak of the aligned crystal resonance. Minor orientation effects

<sup>4</sup> D. Haneman and E. N. Pugh, J. Appl. Phys. 34, 2269 (1963).

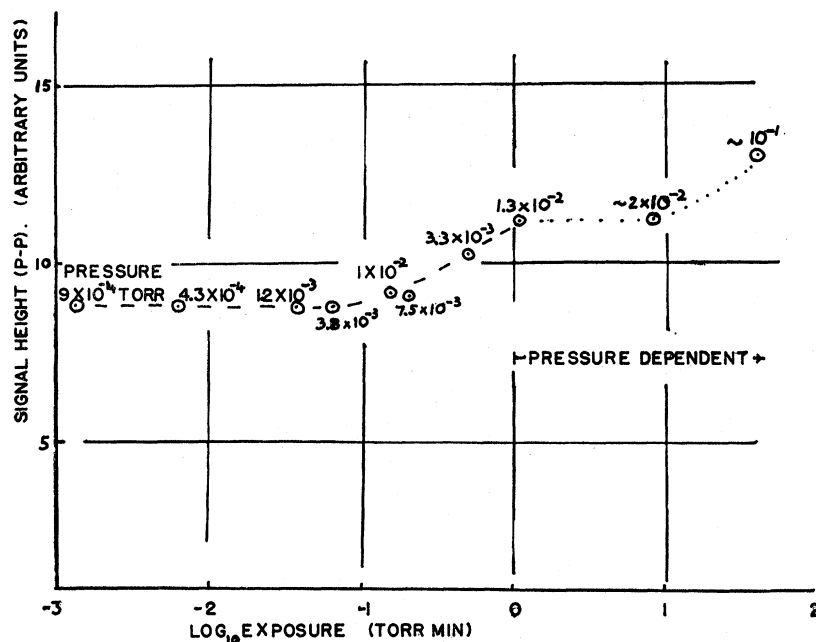


FIG. 6. Graph of signal height versus oxygen exposure. The magnitudes of the last two exposures are partly estimated.

could possibly have been present but would have been below the detectable limits as seen in Fig. 5.

Although the parallelism of the faces was imperfect by a few degrees, the absence of observable rotation changes was not expected; hence the extra precautions described earlier were undertaken to ensure that the resonance originated from the cleaved surfaces.

### B. Adsorption Effects

With the crystals in ultrahigh vacuum and the signal height confirmed by a number of separate accumulations, spectroscopically pure oxygen was admitted by means of an adjustable metal leak valve. The pressure was measured using a thoriated iridium filament of an ionization gauge, which gives minor CO conversion, and only short "on" periods were used. In some low-pressure runs the ion pump was left on to establish dynamic equilibrium pressure conditions. The gauge in its position midway along the tube leading to the EPR tube read a pressure higher by a factor of  $10^2$  than that deduced from the pump current. Neither reading was considered very reliable, but the true oxygen pressure at the crystals was probably well within a factor of 10 of the reading on the gauge. From the nature of the results and their interpretation, higher accuracy was not required at this stage. At higher pressures ( $>10^{-3}$  Torr) the ion pump was left off and in another set of experiments it was left off at all exposures.

The results were that no significant change in the signal took place until cumulative exposures into the  $10^{-2}$ – $10^{-1}$  Torr min range were applied. Pressures were  $10^{-3}$ – $10^{-2}$  Torr. The results are shown in Fig. 6. After a cumulative 3 Torr min, oxygen was let in to an estimated several tenths of a Torr for 10 h, but this ex-

posure is only estimated as "heavy" due to the lack of a suitable manometer in this pressure region. However, the increase in signal in this region appears to be more due to the higher pressure than to the longer time, from inspection of Fig. 6. Pumping out of the oxygen after some of the exposures caused a few percent increase in signal which was not significant within the accuracy of measurement after accumulation (see Sec. III). Similar doubtful small changes occurred after letting in  $H_2$  after the last oxygen exposure and subsequently after letting in air.

It should be noted that the results all refer to gas-covered surfaces in the presence of a magnetic field of about 3000 G. Although these EPR measurements cannot be made without the field, its effect, if any, could be determined by some other measurement technique which does not require a magnetic field. However, we do not know of any evidence that fields of this magnitude do affect the adsorption of  $O_2$  on Si.

The large increases in signal height, up to 45%, were similar to the increases found on exposing vacuum-crushed Si powders to oxygen.<sup>2</sup> The exposures required in the latter case seemed to be somewhat less, by up to factors of 10. A possible reason for the differences, apart from doubts about oxygen pressure measurements, is the effectively higher exposures on powder surfaces exposed to gas trapped in the innumerable interstices in the powder, than in the free space, due to osmotic effects. However, whether for powders or single-crystal cleavages, no effects were noted for exposures less than approximately  $10^{-3}$  Torr min, which will be shown later to be the significant feature.

Because of the noise present even after accumulation and the presence of background signals, very small

changes in linewidth and line shape could not be detected after adsorption. Such small changes were observed in the powder resonances<sup>2</sup> and could have been present here also. Certainly, no width changes larger than approximately 10% took place.

It is of interest to determine the increase in the number of spins after maximum oxygen adsorption. To do this accurately required knowledge of the shape of the resonance near the wings in order to obtain the area under the integrated recorder trace, being proportional to the number of spins. The background was, unfortunately, too large to determine possible changes in the wings. However, from analysis of intense powder resonances,<sup>5</sup> it was possible to show that the change in line shape upon oxygen adsorption could not account for more than a 20% increase in signal height if the number of spins remained unaltered. Assuming that similar considerations apply to the aligned faces, the number of spins increases by at least 20% (signal height up 45%) on oxygen adsorption.

### C. Density of Spins

The number of spins per unit area had previously been estimated from the powders by measuring the surface area using the Brunauer-Emmett-Teller (BET) krypton adsorption method. The use of large cleavages allows a more direct method of area determination by dimensional measurement.

The number of spins was obtained from comparison with a calibrated sample of 0.00033% pitch in KCl, having  $1 \times 10^{13} \pm 25\%$  spins per cm of sample length (3-mm-i.d. tube). After exposure of the Si crystals to air, they were stacked in a separate 6-mm-o.d. open mouthed tube without the carrier, and the resonance was measured with and without the pitch sample tube. The latter was placed inside the 6-mm tube, resting gently on the crystals, and then lifted off. The pitch resonance occurs at  $g=2.0028$  with a linewidth of 1.7 G and causes a hump just beyond the second peak in the Si resonance.

The number of spins was estimated using the relation<sup>6</sup>

$$n_s = \frac{n_p \eta_p \alpha_p C_p A_p (\Delta H_p)^2}{\eta_s \alpha_s C_s A_s (\Delta H_s)^2},$$

where the subscripts  $s$  and  $p$  refer to the Si and pitch, respectively,  $n$  is number of spins,  $\eta$  is the filling factor,  $\alpha$  the transition probability factor,  $C$  the line shape factor,  $A$  the amplitude or peak-to-peak height, and  $\Delta H$  the linewidth. The use of the factor  $CA(\Delta H)^2$  is an approximation to replace integration over the full curve (appearing on the recorder in differentiated form from the true absorption curve, due to the modulation technique of measurement). However, because of background, the cleaved surface signal could not be accu-

rately integrated; hence the commonly employed expression  $CA(\Delta H)^2$  was used. The shape factor  $C$  is 2.73 for pitch in KCl and  $\Delta H$  is approximately 1.7 G. The value of  $C$  chosen for the Si was determined by the shape known for the powder resonance, approximately 2.2, and the linewidth  $\Delta H$  (Fig. 5(b)) was taken as 5.4 G. The ratio of transition probability factors was assumed to be unity, which is expected to be sufficiently accurate for spin- $\frac{1}{2}$  centers.

The filling factor ratio was determined by comparing the signal strength from the silicon with and without the pitch, with that of the pitch when with the silicon. From the values,  $\eta_s/\eta_p$  was approximately 3. Then using the measured Si cleavage surface area of 0.7 cm<sup>2</sup> (to within approximately 20% due to departures from flatness), the density of spins is calculated as  $1 \times 10^{14}$  spins cm<sup>-2</sup>. This applies to air-covered surfaces. The density of spins for the clean surfaces is then obtained from the differences in signal for the clean- and air-covered surfaces. From Fig. 6, the effect of O<sub>2</sub> and air increased the signal height by 45% but a decrease in width of approximately 10% also occurred (known from more intense powder resonances). This therefore yields  $8 \times 10^{13}$  spins cm<sup>-2</sup> for the clean surfaces. The errors in the factors involved in this determination give a cumulative uncertainty of at least a factor of 2 in the result.

The figure of  $8 \times 10^{13}$  spins cm<sup>-2</sup> may be compared with the estimate<sup>2</sup> of  $20 \times 10^{13}$  spins cm<sup>-2</sup> obtained from the clean powders of a 100 times larger area. The uncertainties in this determination were greater due to use of the indirect BET adsorption method to estimate the area. The two estimates nevertheless agree within a factor of 2.5 which is considered good in view of the precision attainable.

## VI. DISCUSSION

The principal features in the results are the following:

- (i) The resonance from clean large aligned cleavage surfaces of Si is similar to that from vacuum-crushed powders, apart from possible small differences in line shape which are below detection limit in the relatively weak cleavage resonance. The resonance is a single line at  $g=2.0055$  of width 6 G.
- (ii) The signal appears to display little, if any, anisotropy.
- (iii) No hyperfine structure from the 4.7% abundant Si<sup>29</sup> is resolved.
- (iv) Oxygen exposures below 10<sup>-3</sup> Torr min have no detectable effect on the resonance.
- (v) Oxygen exposures in the 10<sup>-1</sup> Torr min range increase the signal height, up to 45% for heavy exposures, and increase the number of spins by at least 20%.
- (vi) The density of spins on the clean surface is  $8 \times 10^{13}$  cm<sup>-2</sup>, to within a factor of about 2.

<sup>5</sup> Performed by Dr. M. F. Chung.

<sup>6</sup> W. Jung and G. S. Newell, Phys. Rev. 132, 648 (1963).



We first make a comparison between the resonance from powders and large aligned cleavage faces. The signal appears to be similar. Further, the number of spins per unit area exposed is the same within the limits of measurement. Finally, the resonance increases with oxygen exposure in a similar manner. From this we conclude that the EPR centers produced by minimal stress cleavage, as used here, are the same as those produced during breakup of the silicon by the crushing techniques described previously.<sup>2</sup> This means that the generally higher and more complex stresses applied during crushing do not cause new centers over and above those produced by simple cleavage.

We also observe that points (i) and (ii) are consistent. For if the signal from the aligned faces is largely isotropic and if the sole effect of using a powder is to provide a multiplicity of orientations, the signal from the powder should look similar to that from the aligned faces, as is observed.

#### A. Surface or Bulk Origin of Resonance

A matter of especial interest is whether the EPR centers are located on the very surface, being readily associated with the unpaired bonds expected on an ideal surface, or whether they are perhaps distributed within a small depth from the surface. The most pertinent facts are the following.

(1) The resonance appears on cleavage and is proportional to the surface area that is produced. The surface density of centers measured on a 0.7-cm<sup>2</sup> cleavage area in this work and on up to 120 cm<sup>2</sup> of powder area previously<sup>2</sup> agree within a factor of 2.5, which is encompassed within the errors of the separate determinations.

This shows that the number of centers is proportional to the area of surface produced.

(2) The resonance is unaffected by oxygen (and hydrogen) exposures up to almost 10<sup>-3</sup> Torr min, but the height is increased up to 45% or more by heavy oxygen exposures in the 10<sup>-1</sup>-Torr min range and higher ranges.

This again emphasizes the connection of the resonance with the surface. The effect of the gas could be a direct interaction with centers on the surface or an indirect effect due to altering the charge density on the surface which affects the surface space charge layer in a semiconductor, and hence the occupation probability of states in this space charge region. However, the evidence described below shows that the EPR centers are located on the surface.

Various measurements have been made on high vacuum-cleaved Si surfaces, similar to those used here, enabling direct comparison of results. For such surfaces it has been found that oxygen exposures up to approximately 10<sup>-5</sup> Torr min markedly affect the surface

conductivity<sup>7,7a</sup> and the work function.<sup>8</sup> The effect of oxygen on the cleaved surface is to move the band edges on the surface downward by 0.2–0.4 eV, according to the measurements of Aspnes and Handler,<sup>7</sup> and to increase the work function by 0.5 eV, according to the measurements of Allen and Gobeli.<sup>8</sup> However, such exposures had no detectable effect on the EPR signal. If the signal had been due to internal centers of some kind, the change in their occupation probability due to a barrier height change of about 0.3 eV, as determined by Aspnes and Handler, would have caused a considerable effect on the observed resonance. However, no effect was noted.

While this failure to observe a change in resonance after oxygen exposures, known to strongly affect the surface barrier height, is a principal objection to an internal origin for the centers, there are additional equally cogent objections. After very high exposures, when there is little further change in barrier height, the signal does alter, the signal height increasing by 45% and the number of spins by at least 20%. It seems difficult to understand how centers removed more than a few angstroms from the oxygen could, in the absence of barrier height changes, be sufficiently affected to account for the signal change. However, this is readily understood if the centers are on the surface.

Further evidence comes from the large changes in signal observed after adsorption of less than one tenth monolayer of hydrogen.<sup>2</sup> This has negligible effect on the surface barrier or electrical properties.<sup>9</sup> Hence the large change in resonance must come from centers which can be directly affected by the gas. This also shows that the centers are located at the surface itself.

Recently measurements have been reported on Si crushed in gas ambients and heated in the presence of gases or imperfect vacua.<sup>10</sup> Some similarities in the annealing behavior of the resonance to the Si-A center,<sup>11</sup> an oxygen-vacancy pair, were pointed out. However, the differences from the A center are marked. The Si-A center is clearly anisotropic, with *g* values ranging from 2.0031–2.0093. In the case of the aligned crystals used in this work, the resonance from any normal Si-A centers would be very clearly distinguishable from the observed resonance. No such lines were seen. Furthermore, even if it is assumed that oxygen is involved in some other way, the density of oxygen atoms in floating zone silicon is up to 10<sup>16</sup> cm<sup>-3</sup>, hence a slab of 100 μ depth is required to provide enough centers to account for the observed number of spins. However, the above arguments show that the centers must be on or within about one layer of the surface so that there is insufficient

<sup>7</sup> D. E. Aspnes and P. Handler, *Surface Sci.* **4**, 353 (1966).

<sup>7a</sup> M. Henzler, *Phys. Status Solidi* **19**, 833 (1967).

<sup>8</sup> F. G. Allen and G. W. Gobeli, *Phys. Rev.* **127**, 150 (1962).

<sup>9</sup> D. R. Palmer, S. R. Morrison, and C. E. Dauenbaugh, *Phys. Rev. Letters* **6**, 170 (1961).

<sup>10</sup> T. Wada, T. Mizutani, M. Hirose, and T. Arizumi, *J. Phys. Soc. Japan* **22**, 1060 (1967).

<sup>11</sup> G. D. Watkins and J. W. Corbett, *Phys. Rev.* **121**, 1001 (1961).



oxygen available. Even without this restriction, in the case of the powders<sup>2</sup> the average size of the particles was  $5 \mu$  so that the available number of oxygen atoms, assuming that the entire bulk content was available, was still a factor of 40 lower than the observed number of centers. It is hence concluded that internal oxygen cannot be involved in the line at  $g=2.0055$  due to clean surfaces. (Oxygen may, however, be involved in different resonances produced by heating air covered Si.<sup>2,12,13</sup>)

A search has not revealed any center in Si, due either to impurities or to some kind of radiation damage, which does have the same characteristics as the present line. However, let us consider the possibility that some new kinds of defects, such as, for example, vacancy pairs or other clusters, are produced during cleavage. If this does occur, the gas adsorption results show, as described above, that they would have to be in the surface or within about one layer of it. It does seem difficult to envisage a required concentration of  $\sim 10^{14} \text{ cm}^{-2}$  of such hypothetical centers on the surface. In fact, this type of hypothesis verges onto regarding the surface itself as a sheet of vacancies. It is this which seems the most natural explanation of the source of the unpaired electrons, namely, the dangling bonds present on an ideal (111) surface prior to any possible rearrangement. We therefore proceed to consider this in detail.

### B. Surface Model for Silicon

Principally, two kinds of cleavage facets are produced in cleavage, (111) and (110), in proportions that vary somewhat depending on whether oriented cleavage or random crushing is employed. In the case of the cleaved crystals, one estimates that about 90% or more of the area was (111). This was of course promoted by applying stresses favorable to separation of the material along (111) planes. Micrographs of the cleavage surfaces showed small conchoidal regions plus mainly large flat ones with occasional steps.<sup>4</sup> Cleavage surfaces similar in appearance to those obtained here (Fig. 4) have been found to show intense (111) LEED patterns,<sup>16</sup> indicating that the majority of the surface on a microscopic scale is indeed parallel to (111) planes despite the presence of macroscopically observable steps. During crushing the separation forces are not so well oriented, but the more ready cleavage on (111) planes still causes the majority of the surfaces to display (111) facets. If we assume that the (110) facets are primarily responsible for the resonance, then one needs to assume a density of at least one spin per surface atom to account for the observed number of spins. This seems unreasonably high since some overlap between surface wave functions would be expected to occur. LEED measurements on (110) cleavage faces of Si are not available to help in assessing this possibility, but it

<sup>12</sup> H. Kusumoto and M. Shoji, *J. Phys. Soc. Japan* **17**, 1678 (1962).

<sup>13</sup> P. Chan and A. Steinemann, *Surface Sci.* **5**, 267 (1966).

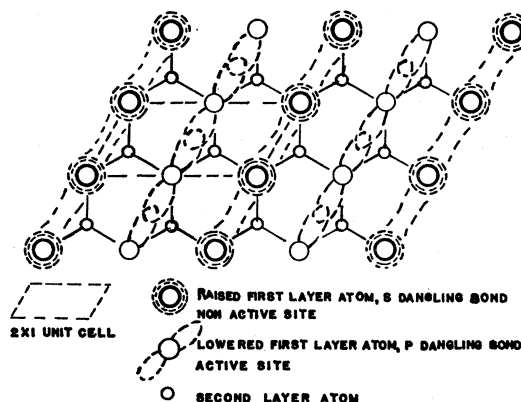


Fig. 7. Model of surface structure of cleaved Si. The alignment of the vertically displaced rows is governed by the direction of propagation of the cleavage crack. The  $p$  and  $s$  terminology indicates partial such content. The unit cell is in accord with LEED measurements (see Refs. 14, 16). Conduction along the  $p$  and  $s$  rows is larger than in the transverse direction.

seems much more reasonable to assume that the (111) surfaces, constituting at least 90% of the available surface, are principally responsible for the resonance, particularly because a more reasonable spin density, 1 per 10 atoms, is then involved. We thus consider principally the properties of (111) surfaces.

A salient feature of the results was the absence of change in the resonance after oxygen exposures of  $10^{-5}$ – $10^{-3}$  Torr min, known to significantly affect the barrier height and work function, but, nevertheless, a subsequent marked change in the resonance occurred when much higher oxygen exposures were applied. This suggests two kinds of atom site on the surface, one not contributing to the resonance but active toward adsorption and one contributing to the resonance but relatively inactive towards adsorption. In this connection it is noteworthy that LEED measurements<sup>14</sup> on vacuum-cleaved Si have shown a rhombus-shaped  $2 \times 1$  unit cell<sup>15</sup> on the surface, rather than the  $1 \times 1$  cell expected from an "ideal" surface. This factor of 2 in the unit cell deduced from LEED data is suggestive when considering the 2-center nature of the surface deduced from the EPR data, and leads us to propose the model shown in Fig. 7 to account for both sets of data.

The model proposed by Lander, Gobeli, and Morrison<sup>14</sup> to account for their LEED data on vacuum-cleaved Ge and Si involved sets of paired atoms. However, this was based on an apparent asymmetry in the [01] direction (indexed with respect to their rectangular  $\sqrt{3} \times 1$  unit cell). Recent measurements<sup>16</sup> on a large number of Ge and Si cleavage faces have, however, shown that asymmetry in this direction is an

<sup>14</sup> J. J. Lander, G. W. Gobeli, and J. Morrison, *J. Appl. Phys.* **34**, 2298 (1963).

<sup>15</sup> Described by Lander *et al.* as  $\sqrt{3} \times 1$ , rotated with respect to the "ideal"  $1 \times 1$  cell. The nonrotated  $2 \times 1$  cell is an alternative description which illustrates more clearly the relationship with the ideal cell.

<sup>16</sup> J. R. Ridgway and D. Haneman (to be published).

artifact. Thus, the paired atom model would require modification. Furthermore, it does not appear able to explain the EPR data, particularly the oxygen adsorption results. A rather different model is therefore required to account for the present EPR data and LEED symmetry results. The LEED data<sup>16</sup> show that the long side of the  $2 \times 1$  cell is in the (112) azimuth direction nearest to the crack propagation direction (which may be different on different parts of the surface), suggesting that the stress wave associated with the advancing crack "pulls" the normal surface structure into this preferred direction on the cleaved face. This finding is consistent with a surface model related to that for the annealed face, to which the cleaved structure reverts on heating,<sup>14,16</sup> except that the annealed structure is aligned or "pulled" into a preferred direction. Using the rumpled surface model<sup>17</sup> as a basis for the annealed surface, as supported by recent work in the case of Ge,<sup>18,19</sup> alignment of the structure along a preferred direction gives the model of Fig. 7. This argument is given to show that the proposed structure is not arbitrary but has a basis in physical reasonableness. The discussion is not in any sense a proof. However, the structure thus deduced is in accord with both the  $2 \times 1$  surface unit cell and the two kinds of surface atom sites. A kinematic type analysis of the LEED data using known methods (performed by D. Miller) gives 0.17 Å for the extra height of the raised atoms and 0.13 Å for the depression of the lowered atoms from their normal heights above the second layer.

Details about the surface bonds were proposed in a previous discussion.<sup>17</sup> Ideally, each surface atom has one dangling bond of average type  $sp^3$ . Following the principle that the surface atoms have fewer neighbors over all and hence the hybridized orbitals tend to show some reversion to their original atomic separate  $s$  and  $p$  nature,<sup>17</sup> one finds that a structure of lowered energy is obtained if some atoms are raised and have  $s$  dangling bonds and if other atoms are lowered and have  $p$  dangling bonds. A natural scheme for this was described earlier,<sup>17</sup> leading to a  $2 \times 2$  unit cell for annealed Ge and Si surfaces, which could be arranged such as to give a  $2 \times 8$  or  $7 \times 7$  structure. Computations using a Morse potential for annealed Ge and Si surfaces have recently shown<sup>20</sup> that this "rumpled" or  $H$ -model structure has lower energy than the "ideal" structure. As described above, we consider the cleaved surface structure to be based on this, only with an alignment or preferred direction caused by the propagating crack which created the surface. This leads to the raised and lowered atoms being arranged in rows as shown in Fig. 7.

In the model the lowered surface atoms have dangling bonds, designated as  $p$  (i.e., intermediate between pure  $p$  and  $sp^3$ ), which strongly overlap with their neighbors in  $[01]$  rows [indexed with respect to the  $2 \times 1$  surface cell shown on the model—the direction is also the intersection of a (112) plane with the (111) surface]. The overlap may be  $\pi$ -type from parallel unpaired bonds or may be enhanced by the bonds having  $[01]$  content; it is sufficient that the overlap be strong enough for any contribution to the resonance to be too small or too broad to be detectable. However, in the presence of oxygen the bond scheme is altered so that the atoms interact strongly with the gas.

The raised surface atoms have dangling bonds designated as  $s$  (i.e., intermediate between pure  $s$  and  $sp^3$ ) which overlap to a degree, but not completely, with their neighbors along  $[01]$  rows. They thus contribute to the resonance. Since there is approximately 1 spin per 10 surface atoms and half of the surface atoms are contributing to the resonance on the model, one assumes that the  $s$  bonds overlap about 80% to give the observed spin density. These bonds do not decouple in a way that would cause strong interaction with oxygen.

Upon adsorption, the oxygen adheres strongly onto the atoms that can make  $p$  bonds available, causing the observed work function and surface barrier changes but not affecting the EPR signal since these atoms were not originally contributing to it. Upon very heavy exposures, however, the oxygen spreads over the entire surface, interacting weakly with the  $s$  bonds which decouple somewhat in the presence of the gas, causing the observed increase in the EPR signal.

This model is also consistent with the formerly puzzling fact that molecular hydrogen adsorbed onto the surfaces with negligible effects on the electrical properties but caused an increase in the EPR signal.<sup>2</sup> The hydrogen is known to interact weakly with Si (heat of adsorption<sup>2</sup> about 35 kcal/mole). We thus assume that it interacts weakly with the partially overlapping  $s$  bonds, causing, as before, some decoupling. This results in an enhancement of the resonance but little change in  $g$ , as observed.

One might have expected that oxygen would interact more strongly with the not fully overlapping  $s$  bands than with the assumed fully overlapping  $p$  bonds. However, this expectation is too simple as the bond character is also important in determining the adsorption characteristics, and after decoupling, the  $p$  bonds may be much more effective than the  $s$  bonds in coupling to the oxygen. Of course, details of the adsorption process are only speculative at this stage of knowledge of oxygen's behavior on surfaces. However, with the above assumption the broad facts are explicable.

### C. Degree of Localization of Centers

According to the model of Fig. 7, the so called  $s$  bonds overlap about 80% in order to account for the observed

<sup>17</sup> D. Haneman, Phys. Rev. **121**, 1093 (1961).

<sup>18</sup> P. W. Palmberg and W. T. Peria, Surface Sci. **6**, 57 (1967).

<sup>19</sup> D. Haneman, W. D. Roots, and J. T. P. Grant, J. Appl. Phys. **38**, 2203 (1967).

<sup>20</sup> A. Taloni and D. Haneman, Surface Sci. **10**, 215 (1968).

spin density of approximately 1 per 10 surface atoms. Since this large overlap occurs equally in either direction along a row due to symmetry, the electrons may not be very localized. This possible expectation can be tested by analyzing the EPR signal on the separate assumptions that the centers are, and are not, well localized. It turns out that only the latter is consistent with the results.

We first comment on isotropy. As described above, there does not appear to be much anisotropy in the present signal. Tests on air-crushed powders show that the width of the resonance increases from 5.4 G at 9.4 Gc/sec (*X* band) to 11.2 G at 35.2 Gc/sec (Ka band).<sup>21</sup> The increase is much less than the frequency ratio, which would yield 22 G, but does suggest the presence of some field-dependent broadening. Since the alignment of the surfaces could have been imperfect, by about  $\pm 5^\circ$ , and cleavage irregularities on the surfaces could have added a small proportion of (111) facets other than those of the cleavage faces, a slight anisotropy might have been spread sufficiently to submerge it in the signal. Nevertheless, it is clear that neither anisotropy nor resolved structure is present to any pronounced degree.

Let us assume initially that the spin centers may be treated as localized and consider the interactions of the neighboring spin sites. We assign in the usual way<sup>22</sup> an effective spin vector  $\mathbf{S}$  to each center and set up an effective spin Hamiltonian for a magnetic field  $\mathbf{H}$ .

$$\bar{H} = \beta \mathbf{H} \cdot \mathbf{g} \cdot \mathbf{S} + \sum_j \mathbf{I}_j \cdot \mathbf{A}_j \cdot \mathbf{S}, \quad (1)$$

where  $\mathbf{S} = \frac{1}{2}$ ,  $\mathbf{g}$  is a tensor measuring the interaction between the field and the component of magnetic moment in the field direction, and  $\mathbf{A}_j$  is the hyperfine tensor measuring the interaction of the spin with the *j*th Si<sup>29</sup> nucleus (4.7% abundant,  $I = \frac{1}{2}$ ). A zero-field splitting term is not included in the Hamiltonian since there is no effect for  $\mathbf{S} = \frac{1}{2}$ , as taken here. We neglect direct Zeeman nuclear interactions.

### 1. Hyperfine Structure

Although hyperfine structure was not resolved, we can at least set upper limits to the amount that might be present though submerged. The linewidth of 5.4 G could encompass hyperfine lines separated by as much as approximately 4 G. We can treat this quantitatively using methods similar to those used by Watkins and Corbett<sup>23</sup> in discussing the Si-*E* center, which is regarded as a dangling bond or unpaired electron adjacent to a vacancy (one of whose four neighbors is a substitutional phosphorus atom). Still treating our surface center as localized, we construct the wave function  $\bar{\psi}$  for the

unpaired electron as a linear combination of atomic orbitals  $\psi$  centered on atom sites:

$$\bar{\psi} = \sum_n \gamma_n \psi_n. \quad (2)$$

At each atom site *n*, counting from the center, we approximate  $\psi_n$  as a hybrid  $3s3p$  orbital given by

$$\psi_n = \alpha_n (\psi_{3s})_n + \beta_n (\psi_{3p})_n, \quad (3)$$

where  $\alpha$  and  $\beta$  are the proportions of *s* and *p* character, respectively, and, ignoring overlap, normalization requires

$$\alpha_n^2 + \beta_n^2 = 1, \quad (4a)$$

$$\sum \gamma_n^2 = 1. \quad (4b)$$

Any combination of *s* and *p* functions must have axial symmetry. Without second-layer distortion, the axis of symmetry would be normal to the surface. However, due to asymmetry of surroundings of the second-layer atoms, some second-layer distortion probably occurs<sup>24</sup> resulting in a tilted axis of surface bond symmetry. To a good first approximation, the hyperfine interaction at the *n*th nuclear site is determined solely by  $\psi_n$ , i.e., by that part of the wave function which is close to the nucleus. In this approximation, and with the hyperfine interaction axially symmetric along the *p* orbital axis, the principal values of the hyperfine tensor may be written

$$\begin{aligned} A_{11} &= \bar{a} + 2\bar{b}, \\ A_{11} &= \bar{a} - \bar{b}. \end{aligned} \quad (5)$$

The isotropic hyperfine term  $\bar{a}$  arises from the Fermi contact interaction

$$\bar{a}_n = (16\pi/3) (\mu_n/I_n) \beta \alpha_n^2 \gamma_n^2 |\psi_{3s}(0)|_n^2, \quad (6)$$

where  $\mu_n$  is the magnetic moment,  $\beta$  the Bohr magneton, and  $I_n$  the spin ( $\frac{1}{2}$ ) of the *n*th nucleus. The anisotropic term  $\bar{b}$  results from the dipole-dipole interaction averaged over the electronic wave function and is given by

$$\bar{b}_n = \left(\frac{4}{5}\right) (\mu_n/I_n) \beta \beta_n^2 \gamma_n^2 \langle r_{3p}^{-3} \rangle_n, \quad (7)$$

where  $\langle r_{3p} \rangle_n$  is the average radius vector of the  $3p$  function at the *n*th nucleus.

Using values of  $|\psi_{3s}(0)|^2$  and  $\langle r_{3p}^{-3} \rangle$  for neutral Si, obtained from the Hartree-Fock calculations of Freeman and Watson,<sup>25</sup> one can then estimate  $\alpha_n^2 \gamma_n^2$  and  $\beta_n^2 \gamma_n^2$  from Eqs. (5)–(7) if the values of  $A_{11}$  and  $A_{11}$  are known. In our case, for a maximum hyperfine line splitting of 4 G, values of  $A$  of approximately  $8 \times 10^{-4}$  cm<sup>-1</sup> are obtained, leading to maximum values of  $\bar{a}$  of similar magnitude. This may be compared with the magnitudes of  $\bar{a}$  and  $\bar{b}$  deduced by Watkins and Corbett<sup>23</sup> for interaction of the unpaired electron with its nearest Si atom (assumed to be Si<sup>29</sup>). Here  $\bar{a} = -115.7$

<sup>21</sup> Measured by N. Gopal Rao.

<sup>22</sup> G. W. Ludwig and H. H. Woodbury, *Solid State Phys.* **13**, 223 (1962).

<sup>23</sup> G. D. Watkins and J. W. Corbett, *Phys. Rev.* **134**, A1359 (1964).

<sup>24</sup> N. R. Hansen and D. Haneman, *Surface Sci.* **2**, 566 (1964).

<sup>25</sup> R. E. Watson and A. J. Freeman, *Phys. Rev.* **123**, 521 (1961).

$\times 10^{-4}$  cm $^{-1}$  and  $\bar{b} = -17.2 \times 10^{-4}$  cm $^{-1}$ , requiring  $\alpha_1^2 = 0.14$ ,  $\beta_1^2 = 0.86$ , and  $\gamma_1^2 = 0.59$ . Clearly, the value of  $\bar{a}$  is about fifteen times less for the surface unpaired electron. Note that in this comparison we have not involved the surface nature of the electron in any way. We have simply set up the wave function as a linear combination of atomic orbitals (LCAO) and compared the experimentally required maximum magnitudes of  $\bar{a}$  and  $\bar{b}$  with those found for an unpaired electron at an internal vacancy. (In the Si-*E* center one of the 4 neighbors of the vacancy is a substitutional phosphorus atom but this has only minor interaction with the unpaired electron<sup>23</sup>).

In order for  $\bar{a}_1$  to be as small as required, we see from inspection of Eq. (6) that the factors  $\alpha^2$ ,  $\gamma^2$ , and, or  $|\psi_{3s}(0)|^2$  must be reduced with respect to those for the *E* center. The 3s density at the nucleus is, however, a calculated atomic quantity,<sup>25</sup> which can be regarded here as a nonvariable. If  $\gamma_1^2$  is left at approximately 0.60, and if  $\alpha_1^2$  is made small, the wave function becomes almost pure *p*. This would lead to a large value of  $\beta_1^2$  and hence to  $\bar{b}_1$  of magnitude requiring an  $A_{11}$  of at least  $50 \times 10^{-4}$  cm $^{-1}$ , which is too large. (Also, an almost pure *p* function would be highly anisotropic.) The only way in which the magnitudes can be accommodated is to assign sufficiently small values for  $\gamma_1^2$ , which is the proportion of the wave function localized on the nearest Si nucleus. Then the approximate value of  $\gamma_1^2$  which is needed is not larger than 0.05, i.e., no more than 5% of the electron density can be localized on the nearest Si atom.

The above calculation therefore shows that if we assume the centers to be localized, the maximum hyperfine splitting that could be present inside the observed line can be accounted for only if less than 5% of the charge density is located on the host atom. Physically, this means that a Si<sup>29</sup> atom that happens to be on the surface would have a hyperfine interaction with an unpaired electron regarded as localized on it, that was detectable unless the degree of localization was less than 5%. Hence the wave function is greatly spread, so that the electron is only slightly localized.

This result, which is of course approximate, agrees quite well with the estimate of 80% overlap of electrons deduced from the measured surface spin density and the model of Fig. 7. It is also in accord with the small *g* anisotropy, as will be shown below.

Another test of the localized electron scheme is to calculate the line broadening due to dipole-dipole interactions. Using the expression derived by Van Vleck<sup>26</sup> for a sample providing all orientations, such as the crushed powder, one has

$$\langle (\Delta H)^2 \rangle = \left(\frac{2}{3}\right) S(S+1) g^2 \beta^2 \sum_j r_j^{-6}, \quad (8)$$

where  $r_j$  is the distance between the center and the *j*th

site. The nearest neighbor on the surface is distant 3.84 Å, leading to a value  $\Delta H = 0.7$  G. This is much too narrow to account for the observations and again indicates that a highly localized electron model is inadequate.

We conclude from the above discussion that the electrons that contribute to the observed resonance are substantially delocalized on the surface. They are thus more akin to conduction electrons. We examine what further information is available from the *g* tensor and observed linewidth.

## 2. *g* Tensor

We first comment further on the question of isotropy. Any localized center which has the symmetry of the host Si lattice would indeed be isotropic, due to the tetrahedral bonding and symmetry of the diamond structure. However, if the centers are on the very surface, the symmetry might be lower for some configurations of the center. Furthermore, despite the possible isotropy in the bulk, one notes that *g*-tensor anisotropy is observed<sup>22</sup> for many kinds of internal defects in Si. Lowering of the tetrahedral symmetry usually occurs for several reasons. Thus the ground state may have orbital degeneracy and undergo a spontaneous (Jahn-Teller) distortion, or a second defect may be situated nearby, or the surrounding crystalline symmetry may be distorted from the cubic symmetry by the presence of the center. Furthermore, in all cases hyperfine structure is usually observed.

However, for the case of bulk conduction electrons, the hyperfine structure is averaged out and observed *g* anisotropy (without strain) is usually very small. This is, therefore, in better accord with the nature of the present results and reinforces the conclusion that one is dealing with surface electrons that are largely nonlocalized.

The *g* tensor for conduction electrons in the bulk in semiconductors has been calculated by Roth<sup>27</sup> on a two-band model. The principal problem is to assign the wave functions and to estimate the spin-orbit coupling which is responsible for the *g* value being different from the free-electron value  $g_0 = 2.0023$ . Since only states in the immediate vicinity of band edges are important, one can ignore the *k* dependence of the *g* tensor and use the effective-mass approximation. For bulk semiconductors Ge and Si, the conduction-band edge consists of several valleys lying in equivalent positions along certain symmetry directions in the Brillouin zone. Hence the spin-orbit interaction introduces an asymmetry into the single-valley *g* value, which can be expressed as a tensor. This anisotropy exists despite the cubic symmetry of the lattice, but because of the latter symmetry the measured value is an average over the cube directions, which is isotropic.

<sup>26</sup> J. H. Van Vleck, Phys. Rev. 74, 1168 (1948).

<sup>27</sup> L. M. Roth, Phys. Rev. 118, 1534 (1960).

In the case of conduction electrons on the surface there would be lower than cubic symmetry and hence some  $g$  anisotropy might be in principle observable, assuming it was not averaged out by the short collision times<sup>28</sup> of the electrons. As indicated previously from the Ka-band results, we believe that there is some small spread in  $g$  values present within the line, possibly associated with different angles between the equivalent (112) azimuth directions (on the surface) and the magnetic field.

In the case of Ge, Roth's<sup>27</sup> two-band model gives results in good agreement with experiment, particularly for  $g_{11}$ , but for Si a more complicated treatment, involving additional contributions from lower lying  $2p$  core states, is found to be necessary.<sup>29</sup> A corresponding treatment for the case of the surface would certainly require modification. However, we can use Roth's simple formula in terms of effective masses, to get at least a feel for magnitudes.

$$g_{11} - 2 = -(\delta/E)(m/m_1 - 1), \quad (9)$$

where  $\delta$  is  $\frac{2}{3}$  of the spin-orbit splitting of the valence band at  $k=0$ ,  $E$  is the difference between appropriate conduction- and valence-band edges, and  $m_1$  is the effective mass in the transverse direction of the energy ellipsoid in  $k$  space. This expression applies better to bulk Ge than to Si. However, applying it as a first approximation to the Si surface, with  $\delta=0.027$  eV as for the bulk,  $E$  taken as about 4 eV for the surface, similar to the bulk, and  $g$  taken as 2.0055, one obtains for  $m_1$ , regarded as a surface effective mass,  $m^*=5m$ . This may therefore be regarded as some indication that the effective mass of the surface conduction electron is large.

The more accurate calculation of the  $g$  tensor for Si conduction electrons by Liu,<sup>29</sup> taking into account  $2p$  atomic core wave function, yields  $(g_{11}-g_0)=-0.0027$  and  $(g_1-g_0)=-0.0036$ . These values agree well with the experimental measurements<sup>30</sup> of  $(g-g_0)$ ,  $-0.0028$  and  $-0.0040$ , respectively, the anisotropy in  $g$  being revealed by applying strain. It is to be noticed that the maximum  $g$  difference is only 0.0012, corresponding to a field separation at  $X$  band of only 2 G. In the case of the surface conduction electrons we do not expect to find a completely isotropic  $g$ , as mentioned before, since there is lower than cubic symmetry. However, according to the model of Fig. 7, there are three equivalent directions in the surface, and although one direction is preferred by the initial crack progression, patches where the crack deflected are usually observed, both from tear mark patterns<sup>4</sup> and from the recent LEED patterns.<sup>16</sup> Furthermore, there are two opposite surfaces, so that the surface is on the average a mirror plane. Hence, with respect to rotation of the magnetic field in the plane of the surface, little average anisotropy is expected. If the

unpaired wave functions do have substantial  $s$  content, as suggested by the model, isotropy is further enhanced. Finally, for field rotation about an axis lying in the surface, which might show the most anisotropy, the results show that the possible unresolved line separation is less than 3 G (from Ka-band comparison above). This is even more than the maximum line separation due to the anisotropy of the bulk wave function along a single axis, which is 2 G.

Hence the failure to observe definite anisotropy means that if any exists it is of no more than about the same magnitude as that along a single bulk axis. However, as described, there is both considerable symmetry in the surface case, and the wave function is expected to have much  $s$  content, so that little anisotropy is expected to be present.

#### D. Linewidth and Temperature Dependence

The linewidths of most bulk centers in Si are in the range 1-2 G.<sup>22</sup> Measurement of the conduction-electron linewidth in Si by Lancaster *et al.*<sup>31</sup> showed considerable temperature dependence, the width (at  $Q$  band) increasing from about 4 G at liquid-nitrogen temperature (78°K) to about 12 G at room temperature. The generally larger linewidths for conduction electrons are thus in accord with the relatively large 6 G ( $X$  band) width ascribed to surface conduction electrons. Although the surface line may have some unresolved structure, the width of the components must also be large to prevent them being resolved.

The aligned samples were too large to permit use of a Dewar in the cavity, for making tests at low temperatures. However, results for the vacuum-crushed powders<sup>2</sup> show a linewidth reduction of only 15% on reducing the temperature from room temperature to the temperature of liquid nitrogen. This may be contrasted with the 66% reduction for bulk conduction electrons.<sup>31</sup> Theoretical treatments of the temperature dependence and of the magnitude of the linewidth are complex and depend on knowing the relaxation mechanisms, but it is not surprising that the surface-line temperature dependence is different from that of the bulk.

For the latter case an estimate by Elliott<sup>32</sup> yields

$$\tau T_1^{-1} \sim (g-g_0)^2, \quad (10)$$

where  $\tau$  is the relaxation time associated with the electrical conductance,  $T_1$  is the spin lattice relaxation time, and  $g_0$  the free-electron  $g$  factor, 2.0023. Use of this formula with  $g=2.0055$  for the surface, instead of 1.9988<sup>29</sup> (for heavily phosphorus doped Si), gives a value of  $T_1$  for the surface which is similar to the bulk theoretical value, since  $(g-g_0)$  is of similar magnitude (0.0032 surface and  $-0.0035$  bulk). This is in accord with the similarly large room-temperature linewidth

<sup>28</sup> G. Feher, Phys. Rev. **114**, 1219 (1959).

<sup>29</sup> L. Liu, Phys. Rev. **126**, 1317 (1962).

<sup>30</sup> D. K. Wilson and G. Feher, Phys. Rev. **124**, 1068 (1961).

<sup>31</sup> G. Lancaster, J. A. Van Wyk, and E. E. Schneider, Proc. Phys. Soc. (London) **84**, 19 (1964).

<sup>32</sup> R. J. Elliott, Phys. Rev. **96**, 266 (1954).

compared to localized centers. However, the temperature dependence predicted by Eq. (10) for the linewidth is  $T^{3/2}$ , since  $\tau \propto T^{-3/2}$  for the bulk. A more complicated formula by Yafet<sup>33</sup> predicts a linewidth temperature variation as  $T^{5/2}$ , which appears to be supported by measurements<sup>29</sup> for the range from liquid nitrogen to room temperature, if the linewidth at 78°K is subtracted from linewidths at higher temperatures. However, understanding of line-broadening mechanisms is not satisfactory<sup>34</sup> at this stage and the extra uncertainty of the surface situation makes more detailed comment difficult.

### E. Surface Conduction

The nonlocalized nature of the unpaired electrons on the surface raises the question of electrical conduction on the surface. In essence, we have a continuous, partially filled band from these electrons and another band from the fully overlapping electrons in the  $p$  bonds (Fig. 7). The conductance properties can therefore be given by a formula applicable to metallic conduction:

$$\sigma_s = n_s e M, \quad (11)$$

where  $M$  is the on-surface mobility. Measurements by Aspnes and Handler<sup>7</sup> on clean Si cleavage surfaces at low temperatures did not detect any on-surface conductance, indicating  $\sigma_s < 10^{-12}$  mho. (The limit may be higher because possible surface irregularities may cause anomalously low measured conductances.) Taking  $n_s$  as  $4 \times 10^{14} \text{ cm}^{-2}$  for the number of electrons in the  $p$  or  $s$  band, one requires

$$M < 2 \times 10^{-8} \text{ cm}^2 \text{ V}^{-1} \text{ sec}^{-1}, \quad (12)$$

which is extremely small. Such a low mobility therefore suggests a high effective mass which is in accord with the estimate made above from the  $g$  value.

It should be pointed out that the model of Fig. 7 implies an anisotropy in the surface conduction band, conduction along the raised and lowered rows being greater than across the rows. The rows are oriented as close as crystallographically possible along the cleavage direction. Therefore the conduction measured along the cleavage direction in the surface should be greater, perhaps much greater, than that measured transversely. The experiments of Aspnes and Handler,<sup>7</sup> however, only involved measurement transverse to the cleavage direction, which would give the smallest conductance. It would therefore be desirable to make measurements in both directions. Hopefully, the longitudinal conductance will be sufficiently larger than the transverse

conductance to be detectable, assuming that a major portion of the surface will be aligned by the cleavage technique used.

### F. Surface States

A final feature of interest is the physical nature of surface states which trap electrons at the surface, leading to excess charge and band bending in the adjacent bulk, due to the excess surface charge field. The electrons which we have been discussing are those which are normally present to fulfill surface-atom neutrality conditions. If extra electrons come to the surface or leave the surface, it appears natural for them to enter or leave the  $s$ -conduction band. This would affect the magnitude of the resonance signal and could be tested by applying a sufficiently strong electric field to the crystal surfaces in the cavity. No such experiment has yet been performed.

If the  $p$  band of Fig. 7 is also able to trap or discharge extra electrons, then there are two bands for the surface states. The high-effective mass deduced for the  $s$  band indicates a narrow energy range for the surface states which are related to this band. One could hypothesize that the  $s$  band and  $p$  band are separated in energy with an energy gap between them, thus providing a specific explanation for the model of two surface-state bands discussed by some authors.<sup>7</sup>

### G. Summary

We have shown that an EPR signal arises from electrons on the surface of high-vacuum cleaved silicon, and that the signal is increased by high exposures to oxygen. The absence of resolvable hyperfine structure and  $g$  anisotropy in the resonance have been analyzed. The results are consistent with the surface electrons being largely nonlocalized, occupying conduction bands of high-effective mass. A specific surface model has been proposed which accounts both for the EPR data and the surface-structure symmetry required by LEED measurements.

### ACKNOWLEDGMENTS

The author is grateful to the National Science Foundation for award of a Senior Foreign Scientist Fellowship, under which the work was performed. He is indebted to Professor H. E. Farnsworth and Professor P. J. Bray for their kind cooperation and for provision of facilities, and to Brown University for hospitality. He has had useful discussions, in particular, with Dr. G. D. Watkins of G. E. Technical and glass-blowing assistance was provided by L. Maigret and M. J. Michael.

<sup>33</sup> Y. Yafet, *Solid State Phys.* **14**, 90 (1963).

<sup>34</sup> G. Lancaster, *Electron Spin Resonance in Semiconductors* (Adam Hilger Ltd., London, 1966).

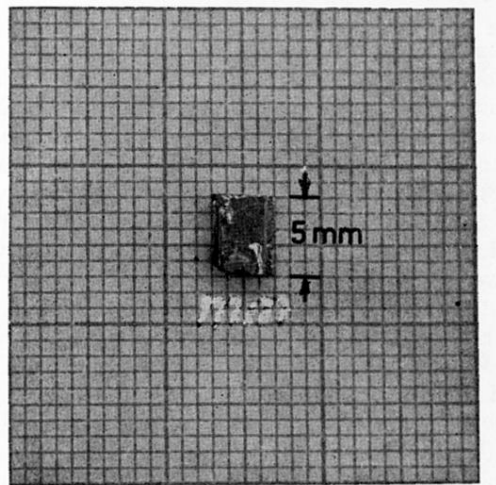


FIG. 4. Photograph of cleavage face showing some steps.